Published in final edited form as:
Pigment Cell Melanoma Res. 2014 November ; 27(6): 1097–1105. doi:10.1111/pcmr.12289.

DNA methylation Profiles in Primary Cutaneous Melanomas are Associated with Clinically Significant Pathologic Features

Nancy E. Thomas[1,2], **Nathaniel A. Slater**[1], **Sharon N. Edmiston**[2], **Xin Zhou**[3], **Pei-Fen Kuan**[2,3], **Pamela A. Groben**[4], **Craig C. Carson**[1], **Honglin Hao**[1], **Eloise Parrish**[2], **Stergios J. Moschos**[2,5], **Marianne Berwick**[6], **David W. Ollila**[2,7], and **Kathleen Conway**[2,8]

[1]Department of Dermatology, University of North Carolina, Chapel Hill, NC, USA

[2]Lineberger Comprehensive Cancer Center, University of North Carolina, Chapel Hill, NC, USA

[3]Department of Biostatistics, University of North Carolina, Chapel Hill, NC, USA

[4]Department of Pathology and Laboratory Medicine, University of North Carolina, Chapel Hill, NC, USA

[5]Department of Medicine, University of North Carolina, Chapel Hill, NC, USA

[6]Department of Medicine, Division of Epidemiology, University of New Mexico, Albuquerque, NM, USA

[7]Department of Surgery, University of North Carolina, Chapel Hill, NC, USA

[8]Department of Epidemiology, University of North Carolina, Chapel Hill, NC, USA

Summary

DNA methylation studies have elucidated a methylation signature distinguishing primary melanomas from benign nevi and provided new insights about genes that may be important in melanoma development. However, it is unclear whether methylation differences among primary melanomas are related to tumor pathologic features with known clinical significance. We utilized the Illumina Golden Gate Cancer Panel array to investigate the methylation profiles of 47 primary cutaneous melanomas. Array-wide methylation patterns revealed a positive association of methylation with Breslow thickness and mutated *BRAF*, a negative association with mitotic rate, and a weak association with ulceration. Hierarchical clustering on CpG sites exhibiting the most variable methylation (n=235) divided the melanoma samples into three clusters, including a highly-methylated cluster that was positively associated with Breslow thickness and an intermediately-methylated cluster associated with Breslow thickness and mitotic rate. Our findings provide support for the existence of methylation-defined subsets in melanomas, with increased methylation associated with Breslow thickness.

Correspondence to: Nancy E. Thomas, MD PhD, Department of Dermatology, University of North Carolina, 405 Mary Ellen Jones Building, CB#7287, Chapel Hill, NC 27599. Phone: (919) 966-0785; Fax: (919) 966-6460; nthomas@med.unc.edu.

Keywords

Melanoma; Primary Melanoma; Methylation; Pathologic Features; Global Methylation Patterns; Methylation Clusters or Subgroups; CIMP

Introduction

Melanoma is an aggressive malignancy that can metastasize early. In addition to somatic mutations, epigenetic alterations are emerging as contributors to melanoma development, potential complementary diagnostic and prognostic biomarkers, and even novel targets for treatments(Greenberg et al., 2012; van den Hurk et al., 2012). The most studied epigenetic changes in melanoma involve hypermethylation at specific sites, commonly in CpG-rich regions of promoters (Hughes et al., 2013). Despite increasing knowledge about the impact of methylation in melanoma biology, little is known about the methylation profiles of primary melanoma specimens. Previously we elucidated methylation differences distinguishing primary melanomas from benign nevi (Conway et al., 2011), but it is unclear if aberrant methylation in melanoma is associated with worse prognostic characteristics or may define a clinically-relevant subtype. Characterizing the relationship between melanoma profiling and well established pathologic and molecular features could shed light on whether methylation has a role in melanoma progression and tumor heterogeneity. This knowledge could also impact selection of methylation markers for primary melanoma diagnostic and prognostic panels.

In other studies, global methylation profiling has associated CpG island methylation in melanoma with progression to brain metastasis(Marzese et al., 2013) and with worse prognosis in stage IIIC patients(Sigalotti et al., 2012). However, limited data has been reported on the association of methylation with melanoma pathologic features or molecular subtypes. *NRAS*-mutation has been associated with *p16INK4A* promoter methylation (Jonsson et al., 2010), and in vitro studies have indicated that *BRAF* mutation may play a role in regulating methylation in melanoma (Hou et al., 2012; Liu et al., 2012). However, an array-based investigation of 24 primary melanomas did not find methylation to be associated with either *BRAF* mutation status or mitotic rate(Gao et al., 2013). Similarly, no association between ulceration and methylation was observed in a set of 98 CpG sites in genes differentially expressed with ulceration in 17 primary melanomas (Rakosy et al., 2013). LINE-1 repeat sequences, which are hypomethylated in melanoma, have also not been shown to be associated with histopathologic factors (Hoshimoto et al., 2012). The finding that melanomas can lose the ability to convert 5-methylcytosine to 5-hydroxymethylcytosine (5-hmc), a first step in the demethylation process, supports a link between methylation and biologic features, as reduced 5-hmc has been associated with increased Breslow thickness, high mitotic rate, and ulceration in primary melanomas, as well as worse tumor stage and lower survival(Lian et al., 2012). Progressive loss of 5-hmc was also observed with increasing dysplasia in melanocytic tumors (Larson et al., 2014). In addition to relationships between methylation and pathologic features, the presence of a distinctly hypermethylated tumor subset in cell lines as well as primary and metastatic melanoma tissue has been suggested by studies showing aberrant hypermethylation at a limited number of gene

promoters and other loci(Tanemura et al., 2009; Tellez et al., 2009). This proposed CpG island methylator phenotype, or CIMP, has been associated with advancing AJCC (American Joint Committee on Cancer) TNM (tumor, regional nodes, distant metastasis)melanoma stage(Tanemura et al., 2009).

In order to investigate whether specific DNA methylation events were associated with tumor progression or subtype, we examined methylation at CpG sites in relation to pathologic features used for AJCC tumor staging(Balch et al., 2009)and tumor *BRAF* and *NRAS* mutation status in a clinically heterogeneous set of well-annotated primary melanomas. Using the Illumina Golden Gate Methylation Cancer Panel 1 array, which allowed for analysis of 1402 CpG sites after quality control filtering, we evaluated the methylation patterns among 47 primary cutaneous melanomas. We explored array-wide methylation patterns according to their associations with Breslow thickness, mitotic rate, ulceration, and tumor mutation status. Differential methylation at individual CpG sites was investigated using univariate and multivariate analyses. Then, in order to determine whether methylation profiles comprise distinct phenotypes, we employed unsupervised hierarchical clustering on the most variable CpGs (n = 235), followed by K means clustering. The resulting methylation-based clusters were then evaluated for associations with pathologic features and tumor mutational status as a first step towards investigating whether methylation may define a clinically relevant subtype.

Results

Melanoma patient and tumor characteristics

We utilized data from 47 formalin-fixed paraffin-embedded (FFPE) invasive cutaneous primary melanomas that had undergone DNA methylation profiling and passed filtering criteria using the Golden Gate array (Conway et al., 2011). Clinical and histologic characteristics (Table 1) included a median Breslow thickness of 3.1 mm (range 0.4–15.0) and a median mitotic rate of 1.0 mitoses/mm^2 (range 0–9), with 38% ulcerated. *BRAF* or *NRAS* mutations were found in 43% and 11%, respectively, of the melanomas mutually exclusive of each other, while the remaining 47% had neither mutation (wildtype). As the group of *NRAS* mutated tumors alone (n = 5) was underpowered for analysis, we focused on *BRAF* mutated tumors. We found that the combined group of *BRAF* and *NRAS* mutated tumors did not change our analyses of mutational status; therefore, we report analyses of mutational status that include *BRAF* mutated and wildtype tumors only (n = 42).

Array-wide methylation patterns associated with pathologic characteristics

Locus by locus univariate analysis of pathologic covariates vs. CpG methylation at all 1402 CpG sites revealed overall association patterns, which are displayed in volcano plots (Figure 1A). Array-wide, Breslow thickness was positively associated with CpG methylation. Methylation levels were also higher in tumors harboring a *BRAF* mutation compared with wildtype. Mitotic rate showed a negative association with methylation, while ulceration was only weakly positively associated with methylation. A pairwise scatter plot of the coefficients for Breslow thickness vs. mitotic rate (Figure 1B) clarifies the opposite methylation trends associated with Breslow thickness and mitotic rate, showing that one

subset of CpGs (upper right quadrant) was significant for a positive association with Breslow thickness, while a different subset of CpGs (left lower quadrant) was significant for a negative association with mitotic rate. This shows that the observed methylation trends for Breslow thickness and mitotic rate were driven by different subsets of CpGs. Similarly, Breslow thickness, when compared to either ulceration or mutation, was characterized by largely different sets of CpGs, as were each of the other attributes when correlated against one another (data not shown). Breslow thickness and mitotic rate were the most correlated of the clinical attributes, with a rho 0.58. Breslow thickness vs. ulceration and mitotic rate vs. ulceration also showed moderate correlation, while the other plots showed weak correlation (data not shown).

CpG loci associated with pathologic characteristics

A limited number of individual CpG loci were found to have differential methylation that was significantly associated with pathologic characteristics in univariate and multivariate analyses. Reported here are CpG sites that were significant at FDR-adjusted q-value < 0.1; additional CpGs with an unadjusted p-value < 0.001 are listed in Table 2. In univariate analysis, methylation levels at four CpG sites were positively correlated with Breslow thickness (unadjusted r-values reported): PTK7_E317_F (r= 0.43), ABCB4_E429_F (r= 0.37), HOXA9_P303F (r= 0.61), and IRAK3_P185_F (r= 0.51). The former three remained significant in multivariate analysis. MMP14_P208_R was negatively correlated with mitotic rate (r=−0.26) in multivariate analysis only. KLK10_P268_R was positively associated with *BRAF* mutation in univariate analysis only (mean β-value +0.35 in tumors with *BRAF* mutation vs. wildtype). No CpG sites were significantly associated with ulceration.

Validation

Technical validation confirming array-based detection of methylation at a small number of significant CpG loci was accomplished by quantitative methylation-specific PCR (Q-MSP) in at least 8 melanoma cell lines and normal human melanocytes (NHM). Q-MSP assays generally validated array methylation levels well (Figure S1).

In order to further query the observed associations between methylation and pathologic features at individual CpG sites, we interrogated The Cancer Genome Atlas (TCGA) database, in which methylation was assayed using the genome-wide Illumina HumanMethylation450 Beadchip array. We analyzed the subset of primary melanomas (n=66), examining methylation at CpG loci within 200 base pairs of the significant CpG loci from the Golden Gate array. A general decrease in methylation in association with mitotic rate in the region of MMP14_P208 was observed. While methylation at select individual CpG sites tended to increase in association with increasing Breslow thickness, methylation at other sites tended to decrease or remain unchanged (data not shown). Overall, the relationship between methylation and either Breslow thickness or *BRAF* mutation status was heterogenous (Figure S2). Primary tumors deposited in TCGA database were larger than our own samples, with Breslow thickness ranging from 1.92mm to 75mm, and only 5 tumors < 4mm in Breslow thickness. In our own samples, 18 tumors had a Breslow thickness < 2mm. In an independent clustering analysis of TCGA melanomas, across all samples (primary and metastatic tumors combined), three robust methylation-based clusters were observed in

consensus non-negative matrix factorization (Broad Institute TCGA Data Analysis Center, 2014a).

In our gene expression analyses, only *CD40* and *IRAK3* showed correlation coefficients of less than −0.5 between methylation and gene expression (data not shown). In correlation of mRNA expression and DNA methylation from TCGA database, across all tumors (primary and metastatic samples), there was at least one CpG site in the regulatory region of each of the top genes from our list except for KLK10 that showed highly significant correlation between methylation and gene expression (Table S1, collated from the Broad Institute TCGA Data Analysis Center, 2014b).

Clustering reveals a hypermethylated melanoma phenotype associated with Breslow thickness

We next investigated whether melanomas clustered into distinct methylation-based subgroups. Exploratory statistics had revealed that most of the CpGs associated with sex were on the X-chromosome. To avoid sex confounding, CpGs on the X-chromosome were removed for the purposes of clustering. Results of unsupervised hierarchical clustering on the remaining 1,327 CpG sites showed epigenetic heterogeneity, but many invariant CpG loci (Figure S3A). Therefore, we limited the analysis to the most variable CpG sites (standard deviation >0.25), which created a panel of 235 CpG sites. Unsupervised clustering on the most variable 235CpG sites, excluding the X-chromosome, identified 3 methylation clusters, with one cluster notably exhibiting high methylation across nearly all loci (Figure S3B).

K-Means clustering was applied to determine clusters more formally, using 3 clusters as suggested by the results from the unsupervised clustering and supported by the Dunn index. K-Means clustering confirmed the presence of a high-methylation subgroup (n=6, Figure 2A). The clusters were designated as high-methylation (HM), intermediate-methylation (IM), and low-methylation (LM), according to the relative overall degree of methylation. We found that these clusters were significantly associated with Breslow thickness and mitotic rate (Figure 2B). Both HM and IM groups had significantly greater Breslow thickness than the LM group after Bonferroni correction (P = 0.048 and 0.048, respectively), though they were not different from each other. Several individual CpG sites, e.g. in *HOXA9* and *IRAK3*, that showed increasing methylation in association with higher Breslow thickness (Table 2) were also among the genes significantly hypermethylated in the HM group vs. other tumor clusters. The IM group had the highest mitotic rate, and was significantly different from the LM group (Bonferroni-adjusted P = 0.016), while the HM group had a broad range of mitotic rates and was not statistically different. While the HM group approached a higher incidence of *BRAF* mutation and the LM group approached a higher absence of ulceration, neither difference was statistically significant (Bonferroni-adjusted P = 0.232 and 0.305, respectively).

Discussion

In summary, array-wide methylation patterns revealed significant trends in association with multiple tumor features. There was a trend toward increased methylation with Breslow

thickness and the presence of *BRAF* mutation (vs. wildtype) array-wide. In contrast, mitotic rate exhibited a negative association with methylation overall. Distinct subsets of CpG sites were differentially methylated in association with each of these tumor features, although a limited number of individual CpGs were significantly associated with pathologic attributes. These include loci in the regulatory regions of genes involved in various functional pathways, including transcription factors important in embryogenesis (*HOXA9*), immune-related signaling molecules (*IRAK3*), and putative tumor invasion enzymes (*MMP14*), per Gene Cards (Rebhan et al., 1998, www.genecards.org). Unsupervised clustering identified the presence of three methylation-defined subsets including a high-methylation cluster. K-means clustering confirmed low-, intermediate-, and high-methylation melanoma clusters; these differed significantly in terms of Breslow thickness and mitotic rate, with the HM cluster exhibiting the highest mean Breslow thickness while the IM cluster was significantly associated with high mitotic rate.

Interestingly, despite a substantial loss of global DNA methylation content in the progression from benign nevus to melanoma, there is a selective acquisition of methylation with tumor progression (Koga et al., 2009). While our results show heterogeneity in the methylation patterns of primary melanomas, the markers most strongly related to prognostic characteristics did not overlap with the most robust CpG markers identified for melanoma diagnosis, most of which exhibited relative hypomethylation in melanomas rather than hypermethylation(Conway et al., 2011). Of the panel of markers that we have previously shown to best discriminate between melanomas and non-malignant nevi, only one (KLK10_P268_R) was identified by the present study, showing an association with *BRAF* in univariate analysis (Conway et al., 2011). *BRAF* mutation has been associated with both hypomethylation and hypermethylation of many genes in melanoma cell lines, and mechanisms underlying these associations have begun to be elucidated (Hou et al., 2012; Liu et al., 2012). However, previous studies have not found different average methylation levels in cell lines or primary melanomas with *BRAF* mutation versus wildtype(Gao et al., 2013; Tellez et al., 2009). Using a sensitive analysis method, our study clarifies that the overall pattern of methylation within primary melanomas tends to be higher in tumors harboring mutated *BRAF*. We found only a weak association of methylated CpG sites with ulceration, consistent with a previous study (Rakosy et al., 2013). Our study also reports a novel association between methylation and the clinical covariates of Breslow thickness and mitotic rate. In addition, the presence of a cluster of primary melanomas remarkable for its high levels of methylation across a large number of variably-methylated CpG sites supports the presence of a CIMP in melanomas, confirming earlier reports based on limited numbers (13 and 15) of methylation markers (Tanemura et al., 2009; Tellez et al., 2009).

Our finding of three-methylation based clusters in melanoma is supported by an independent clustering analysis performed by the Broad Institute. The inverse association between methylation and mitotic rate that we observed was also supported in TCGA primary tumors. While the associations of methylation at specific CpG sites with Breslow thickness and mutated *BRAF* were not observed in TCGA tumors, this may be due to the difference between our own tumor samples, which tended to be thinner and more superficial, and the primary melanoma samples deposited in TCGA, most of which are tumor stage 4b. Furthermore, the CpG sites from the HumanMethylation450 array were not identical to the

CpG sites from the Golden Gate array for our top markers of interest, and methylation trends at individual CpG sites may not always be reflected in the neighboring region. Some correlation of methylation with gene expression was also evident. While the observed methylation differences may serve as useful biomarkers for clinically-relevant pathologic features, it is unclear to what extent variable degrees of methylation differences at individual CpG sites mediate biologic effects.

Our study reports an association of pathologic tumor characteristics with DNA methylation in 47 primary melanomas, based on a panel of CpG sites in the promoter regions of 793 cancer-related genes. Our results raise the question as to whether DNA methylation plays a role in biological mechanisms underlying the observed clinical attributes. We found that the highly-methylated tumor cluster, comprising 6 of the 47 primary melanomas investigated, is associated with increased Breslow thickness; however, further conclusions are limited by the number of tumors in this cluster. Thus, the putative existence of a CIMP, whether it comprises high- and intermediate-methylation subgroups, and the association with mitotic rate remain to be elucidated in larger studies. It is unclear whether HOXA9_P303F and other CpG sites are associated with Breslow thickness because they mark a CIMP with poorer prognostic features, or whether their association with Breslow thickness is independent of a CIMP. Moreover, it is unknown whether CIMP represents a biologically-distinct subgroup or a more advanced set of tumors that has acquired additional genetic and epigenetic changes during melanoma progression. To our knowledge, our study includes the largest number of primary melanomas analyzed using a high throughput platform to investigate methylation patterns at scale. A limitation to our study is that the Golden Gate platform, which is targeted to the promoters of genes with known significance to cancer, is not comprehensively genome-wide, and the sites most relevant to a putative CIMP may be specific to melanomas, rather than universal to cancer. A genome-wide panel could be used in future studies to establish cut-off thresholds for defining methylation-derived subtypes including a melanoma (M)-CIMP. As all array-based data has certain limitations, sequencing approaches could also be used to complement array-based findings. We conclude that methylation is associated with important tumor characteristics, and that methylation profiles support the possibility of three melanoma subtypes including a CIMP, but the methylation events distinguishing these putative subtypes will need to be more fully characterized in a larger set of melanomas using a more comprehensive platform, along with thorough molecular characterization and outcome data.

Methods

Primary melanomas

Primary formalin-fixed paraffin-embedded (FFPE) invasive cutaneous melanomas (n=47) were obtained from the University of North Carolina (UNC) Hospitals Pathology Archives and the University of New Mexico (UNM) Hospitals Pathology Archives as described (Conway et al., 2011). Age, sex, and anatomic site were abstracted from pathology reports. The UNC and UNM Institutional Review Boards approved the study. Five μm-thick tissue sections were cut from each block containing melanoma and were mounted on uncoated glass slides, and a hematoxylin and eosin (H&E)-stained slide of each melanoma was

reviewed by an expert dermatopathologist (PG) to confirm diagnosis, classify histologic subtype, and score standard histopathology features. *BRAF* and *NRAS* mutations were determined as previously described (Thomas et al., 2004, 2007). The dermatopathologist also encircled the tumors on H&E slides to use as guides for manual dissection of melanoma cells, and DNA was prepared as previously published (Thomas et al., 2004, 2007).

Bisulfite treatment of DNA and array-based methylation analysis

Sodium bisulfite conversion and subsequent purification of DNA was performed using EZ DNA Methylation Gold kit (Zymo Research, Orange, CA, USA) according to the manufacturer's protocol. DNA methylation profiling was accomplished using the Illumina Golden Gate Cancer Panel I methylation bead array (Illumina, San Diego, CA, USA) to simultaneously interrogate 1505 CpG loci associated with 807 cancer-related genes as previously described (Conway et al., 2011).

Quantitative methylation-specific polymerase chain reaction (Q-MSP)

Technical validation of *IRAK3* and *HOXA9* methylation was performed in cell lines, due to insufficient DNA remaining from primary tumors. Q-MSP was performed on the Applied Biosystems 7900 HT Fast Real-Time PCR System using Fast Start Universal SYBR Green Master Mix (Roche) with 20ng of bisulfite treated DNA, 200nm of each primer (methylated and unmethylated pairs recorded in Table S2) in a 25 μl reaction with the following cycling conditions: 95°C for 10 minutes, followed by 45 cycles of 95°C for 10 seconds and 59°C for 25 seconds. Quantitative methylation was measured using the fluorescence-based, methylation-specific, real-time PCR data. The calculation of methylation % for each sample relative to 100% methylated control equals $2^{(-\Delta\Delta Ct)}$ multiplied by 100.

Statistical methods

Methylation data were assembled in Genome Studio software (Illumina, San Diego, CA). The methylation level for individual CpGs was represented by the β-value, defined as previously described (Conway et al., 2011). Filtering was performed on a starting set of 48 samples and 1505 CpGs. β-values of CpGs with detection p-value $>10^{-5}$ were considered unreliable(Marsit et al., 2009). We removed 103 CpGs that had >20% unreliable β-values and 1 sample that had >25% unreliable β-values. The final dataset consisted of 1402 CpGs and 47 samples. Subsequent statistical analyses were carried out using R software (http://r-project.org). The array data has been deposited in GEO (accession number GSE54623).

Volcano plots were derived by conducting array-wide locus by locus univariate analysis employing fully supervised methods to plot each pathologic attribute and *BRAF* mutation against β-values for CpG methylation at all 1402 CpG sites. We regressed y on each clinical covariate and plotted the regression coefficients for each clinical attribute against the statistical significance (negative log-p-values) of each coefficient. Scatter plots were constructed by showing correlation of estimated regression coefficients from Breslow thickness vs methylation association analysis against regression coefficients from mitotic rate vs methylation association analysis.

Univariate analysis was used to compare the association between methylation and a pathologic covariate, adjusting for age, gender, and batch effects. In addition to age, gender, and batch, multivariate analysis adjusted for other pathologic covariates considered in this study, in order to confirm that associations between CpGs and pathologic attributes remained statistically significant in the presence of other covariates.

Unsupervised hierarchical clustering analysis using the Euclidean metric and complete linkage was utilized to visualize methylation patterns across the 47 samples on the 235 most variable CpGs (standard deviation > 0.25 and excluding CpGs on the X chromosome). K means clustering was performed to partition the samples into K=3 clusters. The number of clusters K was chosen based on the Dunn index (Dunn, 1973) and the hierarchical clustering tree structure. For the comparison of the clusters with clinical attributes, p-values were computed using the pairwise Wilcoxon rank sum test and adjusted by Bonferroni correction.

Validation using TCGA data

Methylation β-values from the Illumina Golden Gate Cancer Panel I methylation array were validated using quantitative methylation specific PCR (Q-MSP). For TCGA validation data, we downloaded the subset of primary melanoma samples with available methylation and pathologic information of interest that had been deposited in TCGA at the time of submission. In this dataset, methylation was assayed using the genome-wide Illumina HumanMethylation450 Beadchip. Methylation data from primary melanoma samples with recorded Breslow thickness (n = 51), mitotic rate (n = 14), and *BRAF* V600E or V600K (n = 66) was extracted. Methylation beta values from all CpG loci within 500 base pairs of the most significant probes from the Golden Gate array ($q < 0.1$) were collated and plotted against the respective pathologic feature. All CpGs on the Infinium HumanMethylation450 array that were located within 200 bases upstream or downstream of either the HOXA9_P303_F, IRAK3_P185_F, PTK7_E317, ABCB4_E429, MMP14_P208, or KLK10_P268 CpG sites on the Golden Gate array were included in this analysis. The TCGA dataset for cutaneous melanoma is open access, and data are available without restrictions or limitations, as per TCGA publication guidelines. Visualization of methylation trends and calculation of Spearman's rank correlation coefficients were carried out in Microsoft Excel (2010).

Supplementary Material

Refer to Web version on PubMed Central for supplementary material.

Acknowledgments

Financial support: National Cancer Institute grants R33 CA160138, R21 CA134368, R01 CA112243, and P30 CA016086 (Center Core Support Grant). National Institute of Environmental Health Sciences grants P30 ES010126; National Center for Advancing Translational Sciences award UL TR000083; University of North Carolina Chapel Hill's Lineberger Comprehensive Cancer Center Developmental Grant; Holderness Distinguished Medical Scholars Program (Slater), and The Irene and Robert Alan Briggaman Distinguished Professorship (Thomas).

References

Balch CM, Gershenwald JE, Soong SJ, Thompson JF, Atkins MB, Byrd DR, Buzaid AC, Cochran AJ, Coit DG, Ding S, et al. Final version of 2009 AJCC melanoma staging and classification. J. Clin. Oncol. 2009; 27:6199–6206. [PubMed: 19917835]

Broad Institute TCGA Data Analysis Center. Clustering of Methylation: consensus NMF. Broad Institute of MIT and Harvard. 2014a

Broad Institute TCGA Data Analysis Center. Correlation between mRNA expression and DNA methylation. Broad Institue of MIT and Harvard. 2014b

Conway K, Edmiston SN, Khondker ZS, Groben PA, Zhou X, Chu H, Kuan PF, Hao H, Carson C, Berwick M, et al. DNA-methylation profiling distinguishes malignant melanomas from benign nevi. Pigment Cell Melanoma Res. 2011; 24:352–360. [PubMed: 21375697]

Dunn JC. A fuzzy relative of the ISODATA Process and Its Use in Detecting Compact Well-Separated Clusters. Cybernetics and Systems. 1973; 3:32–57.

Gao L, Smit MA, van den Oord JJ, Goeman JJ, Verdegaal EM, van der Burg SH, Stas M, Beck S, Gruis NA, Tensen CP, et al. Genome-wide promoter methylation analysis identifies epigenetic silencing of MAPK13 in primary cutaneous melanoma. Pigment Cell Melanoma Res. 2013; 26:542–554. [PubMed: 23590314]

Greenberg ES, Chong KK, Huynh KT, Tanaka R, Hoon DS. Epigenetic biomarkers in skin cancer. Cancer Lett. 2012; 342:170–177. [PubMed: 22289720]

Hoshimoto S, Kuo CT, Chong KK, Takeshima TL, Takei Y, Li MW, Huang SK, Sim MS, Morton DL, Hoon DS. AIM1 and LINE-1 epigenetic aberrations in tumor and serum relate to melanoma progression and disease outcome. J Invest Dermatol. 2012; 132:1689–1697. [PubMed: 22402438]

Hou P, Liu D, Dong J, Xing M. The BRAF(V600E) causes widespread alterations in gene methylation in the genome of melanoma cells. Cell Cycle. 2012; 11:286–295. [PubMed: 22189819]

Hughes LA, Melotte V, de Schrijver J, de Maat M, Smit VT, Bovee JV, French PJ, van den Brandt PA, Schouten LJ, de Meyer T, et al. The CpG Island Methylator Phenotype: What's in a Name? Cancer Res. 2013; 73:5858–5868. [PubMed: 23801749]

Van den Hurk K, Niessen HE, Veeck J, van den Oord JJ, van Steensel MA, Zur Hausen A, van Engeland M, Winnepenninckx VJ. Genetics and epigenetics of cutaneous malignant melanoma: a concert out of tune. Biochim. Biophys. Acta. 2012; 1826:89–102. [PubMed: 22503822]

Jonsson A, Tuominen R, Grafström E, Hansson J, Egyhazi S. High frequency of p16(INK4A) promoter methylation in NRAS-mutated cutaneous melanoma. J. Invest. Dermatol. 2010; 130:2809–2817. [PubMed: 20703244]

Koga Y, Pelizzola M, Cheng E, Krauthammer M, Sznol M, Ariyan S, Narayan D, Molinaro AM, Halaban R, Weissman SM. Genome-wide screen of promoter methylation identifies novel markers in melanoma. Genome Res. 2009; 19:1462–1470. [PubMed: 19491193]

Larson AR, Dresser KA, Zhan Q, Lezcano C, Woda BA, Yosufi B, Thompson JF, Scolyer RA, Mihm MC, Shi YG, et al. Loss of 5-hydroxymethylcytosine correlates with increasing morphologic dysplasia in melanocytic tumors. Mod. Pathol. 2014; 27:936–944. [PubMed: 24390216]

Lian CG, Xu Y, Ceol C, Wu F, Larson A, Dresser K, Xu W, Tan L, Hu Y, Zhan Q, et al. Loss of 5-hydroxymethylcytosine is an epigenetic hallmark of melanoma. Cell. 2012; 150:1135–1146. [PubMed: 22980977]

Liu D, Liu X, Xing M. Epigenetic genes regulated by the BRAFV600E signaling are associated with alterations in the methylation and expression of tumor suppressor genes and patient survival in melanoma. Biochem. Biophys. Res. Commun. 2012; 425:45–50. [PubMed: 22820187]

Marsit CJ, Christensen BC, Houseman EA, Karagas MR, Wrensch MR, Yeh RF, Nelson HH, Wiemels JL, Zheng S, Posner MR, et al. Epigenetic profiling reveals etiologically distinct patterns of DNA methylation in head and neck squamous cell carcinoma. Carcinogenesis. 2009; 30:416–422. [PubMed: 19126652]

Marzese DM, Scolyer RA, Huynh JL, Huang SK, Hirose H, Chong KK, Kiyohara E, Wang J, Kawas NP, Donovan NC, et al. Epigenome-wide DNA methylation landscape of melanoma progression to brain metastasis reveals aberrations on homeobox D cluster associated with prognosis. Hum Mol Genet. 2013; 23:226–238. [PubMed: 24014427]

Rakosy Z, Ecsedi S, Toth R, Vizkeleti L, Hernandez-Vargas H, Lazar V, Emri G, Szatmari I, Herceg Z, Adany R, et al. Integrative genomics identifies gene signature associated with melanoma ulceration. PLoS One. 2013; 8:e54958. [PubMed: 23383013]

Rebhan M, Chalifa-Caspi V, Prilusky J, Lancet D. GeneCards: a novel functional genomics compendium with automated data mining and query reformulation support. Bioinformatics. 1998; 14:656–664. [PubMed: 9789091]

Sigalotti L, Covre A, Fratta E, Parisi G, Sonego P, Colizzi F, Coral S, Massarut S, Kirkwood JM, Maio M. Whole genome methylation profiles as independent markers of survival in stage IIIC melanoma patients. J. Transl. Med. 2012; 10:185. [PubMed: 22950745]

Tanemura A, Terando AM, Sim MS, van Hoesel AQ, de Maat MF, Morton DL, Hoon DS. CpG island methylator phenotype predicts progression of malignant melanoma. Clin. Cancer Res. 2009; 15:1801–1807. [PubMed: 19223509]

Tellez CS, Shen L, Estecio MR, Jelinek J, Gershenwald JE, Issa JP. CpG island methylation profiling in human melanoma cell lines. Melanoma Res. 2009; 19:146–155. [PubMed: 19441164]

Thomas NE, Alexander A, Edmiston SN, Parrish E, Millikan RC, Berwick M, Groben P, Ollila DW, Mattingly D, Conway K. Tandem BRAF mutations in primary invasive melanomas. J. Invest. Dermatol. 2004; 122:1245–1250. [PubMed: 15140228]

Thomas NE, Edmiston SN, Alexander A, Millikan RC, Groben PA, Hao H, Tolbert D, Berwick M, Busam K, Begg CB, et al. Number of nevi and early-life ambient UV exposure are associated with BRAF-mutant melanoma. Cancer Epidemiol. Biomarkers Prev. 2007; 16:991–997. [PubMed: 17507627]

Significance

We identified an association between prognostic tumor features and DNA methylation in primary melanomas, based on a panel of CpG sites in 793 cancer-related genes. Our findings link methylation with clinically significant pathologic and molecular features in melanoma, raising the question of whether methylation plays a role in the biological mechanisms underlying the observed clinical attributes, or is related to melanoma progression. We report that methylation patterns in primary melanomas fall into three methylation-based clusters, including one cluster remarkable for its high levels of methylation, which lends support to the presence of a CpG island methylator phenotype (CIMP) in melanoma.

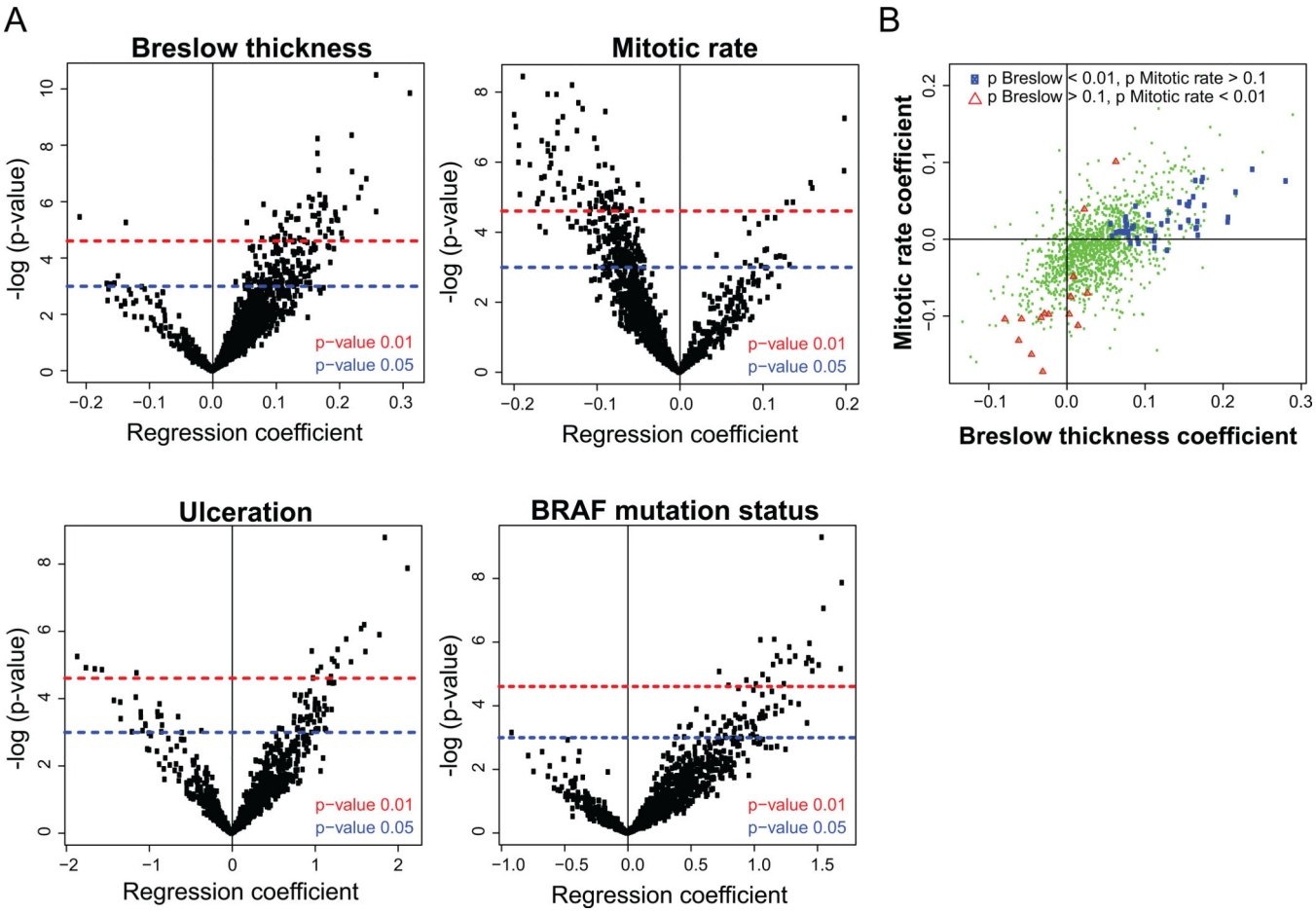

Figure 1. Array-wide patterns of methylation associated with clinical characteristics

Volcano plots were utilized to display array-wide association patterns between methylation and a clinical covariate across all CpGs. Clinical attributes included mutation status in addition to three features used in the AJCC staging of melanoma: Breslow thickness, ulceration, and mitotic rate.

(A) Each point represents a regression coefficient for the covariate vs. methylation level at a particular CpG site, plotted along the x-axis. The y-axis represents statistical significance, with points above the dashed blue line having p-values <0.05, and the dashed red line illustrating the threshold for p-values <0.01.

(B) Scatter plot showing correlation of regression coefficients for Breslow thickness vs mitotic rate indicates that a distinct set of CpGs marks each covariate. Blue circles indicate CpG sites at which the coefficient for Breslow thickness had a p-value < 0.01 while the coefficient for mitotic rate had a p-value > 0.1. Red triangles indicate the converse.

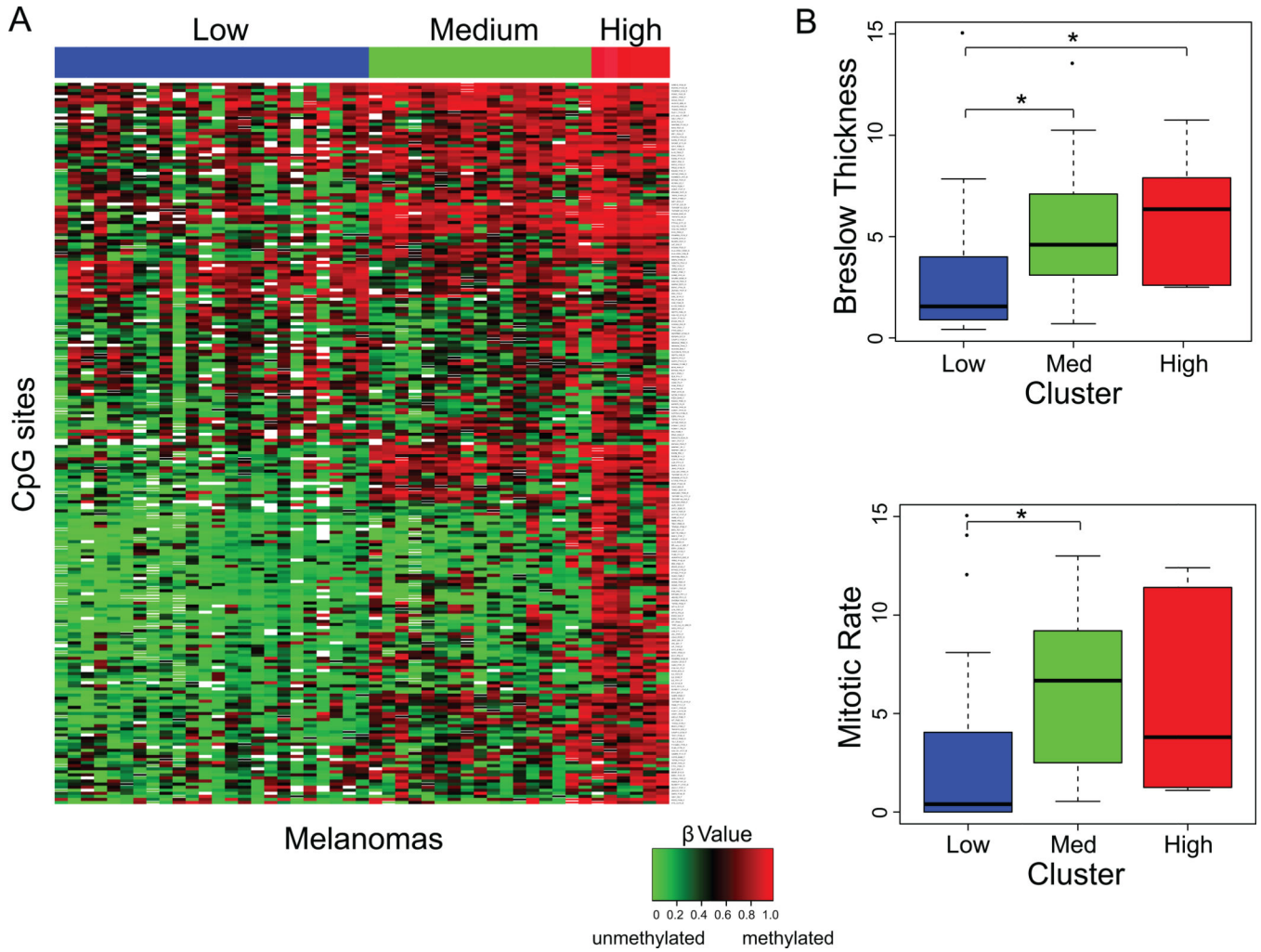

Figure 2. K-means clustering of most variant CpG sites identifies methylation-based subgroups that are associated with Breslow thickness

K-means clustering was performed to partition the samples into K= 3 clusters.

(A) If X chromosome CpGs are excluded, 235 CpGs showed high variability with SD > 0.25. Heat map shows K means clustering of the 235 CpGs with the largest variance across all 47 primary melanoma samples, with K = 3 based on the unsupervised clustering results. Samples are in columns and CpG sites are in rows. Red indicates methylated, green indicates unmethylated.

(B) Clinical attributes are plotted against the 3 subgroups defined by K-means clustering. Dark lines = medians. Pairwise comparison showed that both medium- and high-methylation clusters were significantly associated with Breslow thickness, while the medium cluster was significantly associated with mitotic rate (*Bonferroni-adjusted P < 0.05).

Table 1

Overall demographics along with clinical and histologic characteristics of 47 primary melanomas evaluated for DNA promoter methylation

Characteristic	Melanomas N = 47 n (%)
Sex	
Male	23 (49)
Female	24 (51)
Age	
Median (range)	56 (38–72)
Anatomic site	
Head/neck	12 (26)
Trunk	19 (40)
Extremity	16 (34)
Melanoma histologic subtype	
SSM	23 (49)
NM	5 (11)
LMM	5 (11)
ALM	5 (11)
UNCL, SC	9 (19)
Breslow thickness (mm)	
Median (range)	3.1 (0.4–15.0)
Ulceration	
Absent	28 (60)
Present	18 (38)
Indeterminant	1 (2)
Mitoses	
Median (range)	1.0 (0–9.0)
Mutation	
Wildtype	22 (47)
BRAF	20 (43)
NRAS	5 (11)

Abbreviations: SSM; superficial spreading melanoma, LMM; lentigo maligna melanoma, NM; nodular melanoma, ALM; acral lentiginous melanoma, SC; spindle cell melanoma, UNCL; unclassifiable melanoma, na; not applicable.

Table 2

CpG sites Differentially Methylated in Association with Pathologic Characteristics, P-value < 0.001

Breslow Thickness				
Probe ID	***Univariate*[1]**	***Multivariate*[3]**	***Pearson Coefficient*[3]**	
HOXA9_P303_F*	4.68E-05*	2.74E-05	.609+	
PTK7_E317_F*	0.000115*	0.000186	.434	
ABCB4_E429_F*	0.000151*	0.000192	.371	
IRAK3_P185_F*	0.000157	0.000319	.507	
GNG7_E310_R	0.00036	0.000582	.238+	
HOXA9_E252_R	0.000588	0.00094	.530	
RUNX1T1_E145_R	0.000767	0.001953	.277	
Mitotic Rate				
Probe ID	*Univariate*	*Multivariate*	*Pearson Coefficient*	
+ USP29_P282_R	0.00086	0.000272	−.476	
MMP14_P208_R	0.017198*	6.33E-05	−.265	
SEMA3A_P658_R	0.013546	0.000228	−.272	
AATK_P709_R	0.038656	0.000293	−.0825	
UGT1A7_P751_R	0.017396	0.000551	−.453	
SHH_P104_R	0.006076	0.000566	−.281	
Ulceration				
Probe ID	*Univariate*	*Multivariate*	*Mean Beta Value: Ulceration Present*	*Mean Beta Value: Ulceration Absent*
MAP3K1_P7_F	0.000964	0.005689	0.717439	0.378613
BRAF Mutation[4] vs. Wildtype				
Probe ID	*Univariate*	*Multivariate*	*Mean Beta Value: Mutated BRAF*	*Mean Beta Value: Wildtype*
+ KLK10_P268_R	* 3.14E-05	0.000294	0.523963	0.220489
CD40_E58_R	0.000747	0.00028	0.470448	0.17565
DNMT3B_P352_R	0.001091	0.000612	0.254696	0.122829
+ SEMA3B_P110_R	0.001328	0.000895	0.554509	0.259127

[1] Univariate analyses were conducted using linear models on logit transformed β methylation values to assess the association between methylation (outcome) and each clinical covariate (predictor), adjusting for age, gender, and batch.

[2] Multivariate analyses were further performed to assess if the association remained significant in the presence of other clinical covariates.

[3] Pearson correlation of raw β-value (non-logit transformed) reported. Similarly, raw mean β-value differences are reported.

[4] *BRAF* mutation compared to wildtype only; *NRAS* positive tumors (n=5) excluded.

* when adjusted for false discovery rate, q-value < 0.1

+ previously published as significantly differentially methylated between melanomas and benign nevi (Conway et al., 2011)